Critical current measurements of Nb_3Sn superconductors: NBS contribution to the VAMAS Interlaboratory Comparison*

L.F. Goodrich and S.L. Bray

Center for Electronics and Electrical Engineering, National Bureau of Standards, Boulder, Colorado 80303, USA

Received 7 July 1988

Critical current measurements on several Nb_3Sn superconductors were made as part of an interlaboratory comparison (round robin). These measurements were made in conjunction with twenty-four laboratories from the European Economic Community, Japan and the USA as part of the Versailles Agreement on Advanced Materials and Standards (VAMAS). The results of the NBS measurements, including the effect of sample mounting techniques on the measured critical current, are given. A systematic study of the effect of measurement mandrel (tubular sample-holder made from G10 fibreglass–epoxy composite) geometry revealed that a seemingly small change in that geometry can result in a 40% change in the measured critical current at a magnetic field of 12 T. Specifically, the radial thermal contraction of the measurement mandrel depends on its wall thickness and, thus, so does the conductor prestrain (at 4 K) and, ultimately, the measured critical current. Techniques for reducing variation in the measured critical current are suggested.

Keywords: critical currents; superconductors; Nb_3Sn; VAMAS; NBS

The measurements reported here represent the NBS contribution to a collaborative effort involving twenty-four laboratories from the European Economic Community, Japan and the USA under the Versailles Agreement on Advanced Materials and Standards (VAMAS). The purpose of this effort is to develop critical current (I_c) measurement techniques for Nb_3Sn superconductors that yield consistent results at different laboratories. These were part of an interlaboratory comparison (round robin) where each of the participating laboratories was supplied with samples of three different conductors that had been reacted in various coil geometries to match the I_c measuring instruments of the various laboratories. Each laboratory then measured the I_c of the three samples at several applied magnetic field strengths and two orientations (parallel and antiparallel to the sample coils' self field). Preliminary comparisons of the laboratories' results showed a large variation in the measured critical current. In response, the NBS study was expanded to address specific measurement variables that might have resulted in these discrepancies. The analytical benefit of round robin collaborations is evidenced by these results where the interlaboratory comparison of data demonstrated that a subtle measurement variable can result in a large difference in the measured I_c.

General considerations for accurate critical current measurements have been given[1,2]. The predominant variables that affect critical current measurements of Nb_3Sn wires fall into four categories: sample reaction conditions, measurement mandrel (sample holder) material and geometry, the method used for bonding the sample to its mandrel and damage incurred during shipping or in transferring the sample from the reaction mandrel (tubular stainless steel sample holder) to the measurement mandrel. In the latter three categories, it is the sensitivity of Nb_3Sn to mechanical strain that results in variations in the measured I_c[3]. For these measurements, like samples were reacted at a central location under presumably the same conditions; consequently, the reaction variables were not suspected of being a significant factor. However, in order to address the question of shipping damage, specimens of each sample were reacted and measured at NBS; thus, some measure of the conductor's sensitivity to reaction conditions was obtained. The measurement mandrel material and geometry can work in conjunction with the sample bonding technique to create a dominant measurement variable, the axial strain of the conductor. Under a condition where 1, the circumferential thermal contraction of the measurement mandrel is greater than the axial thermal contraction of the conductor, and 2 the bonding method creates a strong coupling between the sample and the measurement mandrel, significant axial strain of the conductor at 4 K may result. It was discovered in this study that the

*Publication of the National Bureau of Standards, not subject to copyright

0011-2275/89/070699-11 $03.00

circumferential thermal contraction of the G10 fibreglass–epoxy tubes used for the measurement mandrels in this study depends on the tube's geometry, owing to its composite structure. In particular, the ratio of the tube's wall thickness to its radius strongly affects its thermal contraction. Based on these observations, a systematic study of the effect of G10 measurement mandrel geometry on the measured critical current was made.

For the measurement mandrel study, a filled epoxy adhesive was used for bonding the sample to the mandrel. This technique ensured the strong bond and rigid coupling between the sample and mandrel that is necessary for positive stress transmission. In one case, varnish was used as the sample mounting adhesive to study the effect of the Lorentz force on the critical current of a weakly constrained sample. Another variable that depends on the bonding technique is the thermal coupling between the sample and the liquid helium bath. Although a complete epoxy coating of the sample results in uniform mechanical constraint, it also presents a thermal impedance that in some cases may cause a lower measured critical current.

The purpose of the measurements presented here is to document and better understand the sources of inconsistencies in the measured critical current of Nb_3Sn conductors. This understanding is ultimately necessary for determining a consistent and practical unified measurement method. In theory, a measurement method that would give consistent results is easily achieved by imposing extensive constraints on all aspects of the measurement; however, this approach is impractical considering the variety of I_c measurement systems that are presently in use. Consequently, a practical measurement method should impose the least number of constraints that yield acceptable results.

More challenging than the issue of consistent measurements is that of correct measurements. The basic problem that these round robin tests reveal is that the correct and/or best method for critical current measurements of Nb_3Sn is unclear. Thus, a statement regarding the accuracy of these measurements is currently inappropriate. A future joint publication on the results from all participants is planned.

Samples

In order to avoid the identification of commercial products by the manufacturer's name, the samples measured in this round robin will be identified by letter only. Some physical data are provided to indicate the general type of conductor used in these tests.

Sample X had a wire diameter of 0.68 mm and 37 sub-bundles each containing 150 Nb filaments. The conductor fabrication method was an internal tin diffusion process. A single diffusion barrier of Ta separates the filament region from the outer layer of Cu. The sample reaction temperature was 700°C for 48 h.

Sample Y had a wire diameter of 1.0 mm and 7 sub-bundles each containing 721 Nb filaments. The conductor fabrication method was a bronze diffusion process. Each sub-bundle had a Nb diffusion barrier and the matrix was a CuSnTi alloy. The sample reaction temperature was 670°C for 200 h.

Sample Z had a wire diameter of 0.80 mm and 114 sub-bundles each containing 54 NbTa filaments in a bronze matrix. The conductor fabrication method was a bronze diffusion process. The Cu stabilizer was located at the centre of the wire separated by a Ta barrier. The sample reaction temperature was 700°C for 96 h.

Specimens of each sample were heat treated (reacted) at their central laboratory (central reaction). Other specimens of each sample were to be reacted at each individual measurement laboratory (self reaction). A comparison of results from these two groups gives an indication of reaction and shipping variables. Each specimen was reacted on a stainless steel tube that had a spiral groove on it to define the coil pitch. The surface of the stainless steel had been oxidized to reduce the chance of diffusion bonding between the sample and the reaction mandrel. When bonding does occur, the sample can be damaged when it is removed for mounting onto the measurement mandrel. The self reactions performed at NBS were done in a three-zone, vacuum tube furnace. The temperature of the furnace was controlled during the reaction to a precision of $\pm$ 5°C. The furnace temperature calibration was checked and was accurate to $\pm$ 10°C.

Experimental details

The measurement mandrels were constructed from a G10 tube that had a cylindrical copper current contact rigidly attached to each end. Each contact had a superconductive bus bar (Cu and Nb_3Sn tape) connected to it. The sample was transferred from the reaction mandrel onto the measurement mandrel by carefully unthreading the sample from the reaction mandrel and slipping it on to the measurement mandrel (not grooved). The one current contact that was removed for this transfer was then reattached to the measurement mandrel and the sample was tightened onto the mandrel. Each end of the sample was then soldered onto its current contact. An effort was made to avoid a complete superconductive loop formed by the sample and bus bar around the current contact. This was done in order to avoid persistent currents. Three pairs of adjacent voltage taps were placed along the centre of the sample. Each pair had a separation of about 10 cm and there was a 1–2 cm gap between adjacent pairs. The sample was bonded to the mandrel with filled epoxy (or varnish in one case) and allowed to cure. The epoxy coat was kept thin to enhance the thermal conductivity from the sample to the helium bath. This unit was then mounted onto the test fixture where the electrical connections were completed.

The measurements were made at about 4.2 K in a 12 T, 12.7 cm diameter superconductive solenoidal magnet, which has a homogeneity of $\pm$ 0.2% over the region spanned by the voltage taps. Since the ambient atmospheric pressure at this test site is low, resulting in an equilibrium liquid helium temperature of 4.0 K, the dewar pressure was elevated. The pressure in the helium dewar was controlled with a diaphragm-type manostat and the temperature was deduced from the measured pressure. A heater on the bottom of the helium dewar was used to remove the natural stratification and bring the bath into equilibrium at the elevated pressure.

The voltage–current curves for all three voltage tap pairs were recorded simultaneously with a digital processing oscilloscope. An analogue nanovoltmeter with an

amplified output was used to measure the sample voltage of each tap pair. A battery powered current supply was used for the sample current[4]. The sample voltage was measured at numerous sample currents. These points along the voltage–current curve were analysed to determine I_c. The measurements were made with forward (antiparallel magnetic fields, Lorentz force in) and reverse (parallel magnetic fields, Lorentz force out) current directions to determine the effect of self-field and sample-to-mandrel bonding (strain effect). Unless otherwise stated, the I_c values given are averages over all taps, observations and current directions at an electric field strength criterion of 10 μV m^{-1}. The precision of the I_c measurement was about $\pm 0.2\%$.

Another parameter that was determined during the I_c measurement is n. The parameter n is defined by the approximate voltage–current relationship,

$$V = V_o(I/I_o)^n$$

where I_o is a reference critical current at a voltage criterion V_o, V is the sample voltage, I is the sample current, and n reflects the shape of the curve with typical values from 20 to 60 (a higher number means a sharper transition). A lower value of n can be an indication of sample damage or strain.

Some specimens were difficult to measure because they would quench (thermal runaway into the normal state) at relatively low sample voltages (electric field strength about 10 μV m^{-1}). This resulted in some variation in the I_c values due to the small voltage range that could be analysed. In some cases this low quench level was traced to damaged segments (weak links) adjacent to a current contact. These weak links may have been due to sample damage introduced in removing the sample from the reaction mandrel, transferring the sample to the measurement mandrel, or by strain in the transition length near the current contact. The transition between the contact and the G10 has two intrinsic problems. One problem arises from the differential thermal contraction between the contact and the G10, which causes a stress concentration. The other problem is the differential contraction between the copper contact and the sample, which introduces additional sample pre-stain. Difficulties in measuring the Z sample may have been due to its high current density (535 A mm^{-2} at 10 T) and bronze surface layer (larger contact resistance) causing sample heating.

Results

Sample X

A summary of the data on sample X is given in *Table 1* and *Figures 1–4*. The information contained in *Table 1* is the critical current data, sample mandrel dimensions and intercomparisons of critical current data. The critical current data are given at magnetic fields from 6 to 12 T. The effect of sample mandrel geometry, bonding method, thermal cycle, and central or self reaction variables were studied. *Table 1* contains key words that relate to these variables. Each column, which is labelled with a letter from A to G, is a data set taken for a single thermal cycle. Specimens are numbered from 1 to 4. Different data columns that are for the same specimens (columns A and B for example) indicate a thermal cycle where the specimen was measured at 4 K, warmed to room temperature, cooled again to 4 K and remeasured. In some

Table 1 Data on sample X; critical current for sample X

Specimen	1	1	1	2	3	3	4
μ_oH(T)	Central thick (A)	Central thick (B)	Central thin bored (C)	Central thin (D)	Self thin spiral (E)	Self thin (F)	Self thin varnish (G)
6	343.3	343.2	397.3	386.3	388.9	386.6	374.5
7	268.4	267.6	318.4	308.9	312.4	310.3	297.9
8	207.0	207.4	253.8	246.0	249.7	247.6	235.9
9	156.5	156.6	200.1	193.5	197.4	195.6	184.8
10	113.6	114.0	154.7	149.3	153.2	151.6	142.1
11		78.5	116.0	111.9	114.6	112.8	106.6
12		50.2	83.5	80.4	82.5	81.1	74.6
	Sample mandrel dimensions						
	(A)	(B)	(C)	(D)	(E)	(F)	(G)
Wall (mm)	9.3	9.3	2.5	2.0	1.5	1.5	2.0
Rad. (mm)	15.6	15.6	15.6	15.6	15.6	15.6	15.6
w/r	60%	60%	16%	13%	10%	10%	13%
	Intercomparison of critical current data						
μ_oH(T)	Delta (A–B)/B	Delta (B–C)/C	Delta (C–D)/D		Delta (E–D)/D	Delta (F–D)/D	Delta (G–D)/D
6	0.0%	−13.6%	2.8%		0.7%	0.1%	−3.1%
7	0.3%	−16.0%	3.1%		1.1%	0.5%	−3.6%
8	−0.2%	−18.3%	3.2%		1.5%	0.7%	−4.1%
9	−0.1%	−21.7%	3.4%		2.0%	1.1%	−4.5%
10	−0.4%	−26.3%	3.6%		2.6%	1.5%	−4.8%
11		−32.3%	3.7%		2.4%	0.8%	−4.7%
12		−39.9%	3.9%		2.6%	0.9%	−7.2%

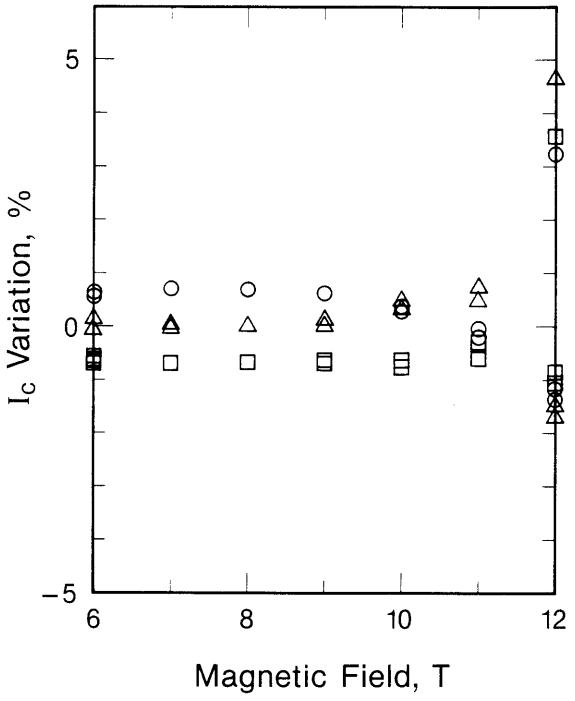

Figure 1 Percentage variation of I_c about the average I_c *versus* magnetic field for specimen G (self, thin, varnish) of sample X. Tap symbols: ○, 1; □, 2; △, 3

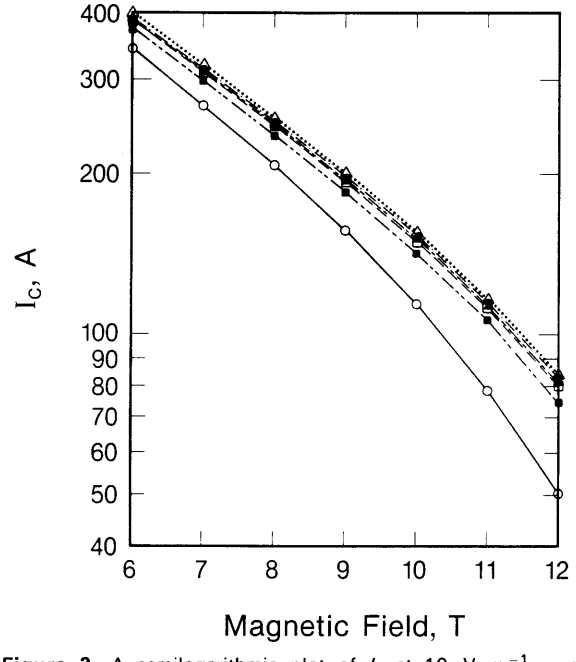

Figure 2 A semilogarithmic plot of I_c at 10 μV m^{-1} *versus* magnetic field for specimens of sample X. $E_c = 10\ \mu V\ m^{-1}$. ○——○, Central thick; △ · · · △, central bored; □ - - - □, central thin; ● - · - ●, self thin spiral; ▲ — — — ▲, self thin; ■ — — — — ■, self thin varnish

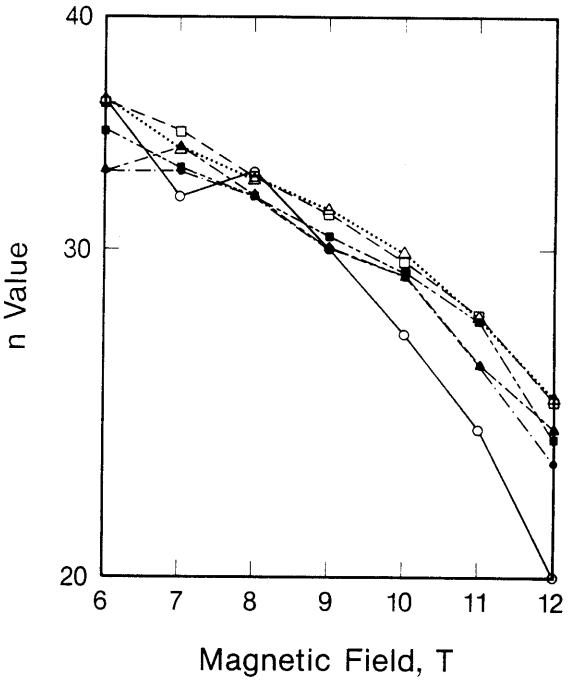

Figure 3 A semilogarithmic plot of *n* value *versus* magnetic field for specimens of sample X. ○——○, Central thick; △ · · · △, central bored; □ - - - □, central thin; ● - · - ●, self thin spiral; ▲ — — — ▲, self thin; ■ — — — — ■, self thin varnish

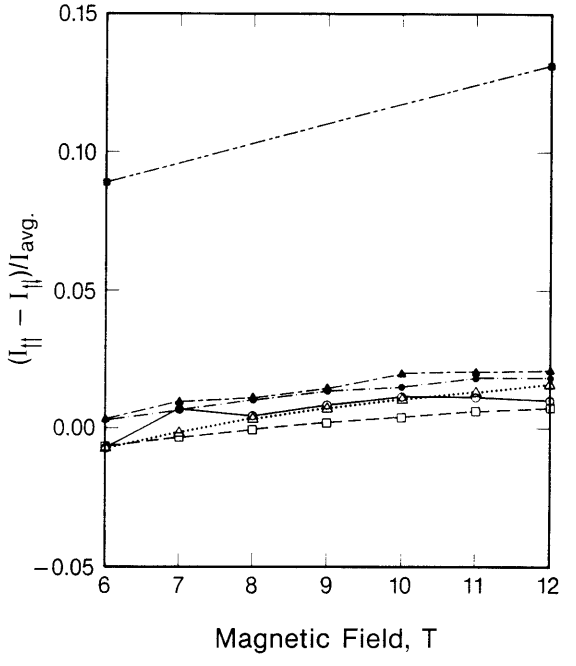

Figure 4 Percentage difference between I_c measured with reverse and forward current directions *versus* magnetic field for specimens of sample X. $E_c = 10\ \mu V\ m^{-1}$. ○——○, Central thick; △ · · · △, central bored; □ - - - □, central thin; ● - · - ●, self thin spiral; ▲ — — — ▲, self thin; ■ — — — — ■, self thin varnish

cases, the mounting configuration of the specimen was changed between these measurements (columns B and C for example). The sequence of the thermal cycles was from left to right in the table.

The key words heading the columns of *Table 1* (central, thick, thin, etc.) are used to indicate the measurement variables. Central indicates reaction of the specimen at a central laboratory and self indicates reaction at the individual measurement laboratory. Thick and thin refer to the ratio of wall thickness to outer radius of the sample mandrel. Under the Sample Mandrel Dimensions section of the table, these specific values are listed for each data set. Bored refers to a specimen that was originally mounted and measured on a thick-walled mandrel. The

specimen was then brought to room temperature (thermally cycled) and the mandrel inner diameter was bored to a larger dimension, resulting in a reduced wall thickness. The specimen's I_c was then remeasured. The typical method for bonding samples to measurement mandrels was to coat the sample and the entire surface of the mandrel with epoxy. Two variations of this technique are indicated by spiral and varnish. Spiral indicates that the sample was bonded to the mandrel with a thin stripe of epoxy along its length. Varnish indicates that the sample and the mandrel were completely coated with varnish rather than epoxy.

The centrally reacted specimens were numbers 1 and 2. A comparison of the I_c data in columns A and B is a measure of the I_c variation due to thermal cycling. The maximum variation was 0.4% at 10 T (the highest magnetic field for column A) as shown in the intercomparison portion of the table ([A–B]/B). This small variation upon thermal cycling was representative of all observations. Column C was a special case of a thin-walled mandrel in that it was bored (machined with the specimen mounted on the mandrel). Because this was the same specimen as A and B, the comparison is a systematic one. The intent of this procedure was to determine the effect of mandrel wall thickness on the measured I_c of a particular specimen. The intercomparison data ([B–C]/C) shows a strongly field dependent variation of I_c (indicative of a strain effect) with a maximum difference of 39% at 12 T. This is believed to result from a change in the conductor pre-strain (at 4 K) due to variation in thermal contraction between thick and thin walled G-10 tubes. An approximate measure of the thermal contraction (from room to liquid nitrogen temperature) variations indicated a 0.2% greater contraction for the thick-walled tube. Strain sensitivity measurements on this sample indicate that this additional pre-strain would result in an I_c degradation in the order of 33%. The composite nature of G-10 plate[5–7] in conjunction with the compound geometry of a tube may result in a variation in radial thermal contraction between tubes of different wall thickness. Machining may have changed the mandrel's outer diameter at room temperature due to stress relief and, thus, the pre-strain state of the conductor. More details regarding thermal contraction of G-10 measurement mandrels and the resulting critical current degradation due to axial strain are presented below. The rest of the intercomparisons in *Table 1* were made relative to D (central, thin) since it was thought to be a more ideal baseline for comparisons. The comparison between C and D showed only a small difference, 3–4%, with very little field dependence ([C–D]/D). This indicates that the effect of boring was about equivalent to that of simply mounting a specimen on a thin-walled tube.

The self reacted specimens on thin wall tubes were numbers 3 (E and F) and 4 (G). For data set E the specimen was bonded to the mandrel with a thin stripe of epoxy along its length (spiral). This spiral mounting technique was employed to examine the effect of a less rigid containment structure. The comparison between D and E was within 2.6%. Furthermore, the comparison of F (E with a continuous epoxy coat) with D was indicative of the small difference, 1.5%, between central and self reacted wires. The systematic difference between E and F was, thus, 1.7% or less. This demonstrates that a continuous epoxy coat was not very detrimental in this case. Specimen 4 (G) was bonded to the mandrel with a coat of varnish in order to investigate the bonding properties of a weaker and less permanent adhesive. The I_c values in column G were averages of data taken with forward current only (Lorentz force into the mandrel). Some measurements were made with reverse current (Lorentz force away from the mandrel) at 6 and 12 T but these results were not included in this table. For this data set, the 12 T (magnetic field of lowest Lorentz force) measurements were made first to reduce the possibility of irreversible strain damage. However, even at this relatively low Lorentz force, there was an irreversible shift in the forward I_c after the reverse I_c measurements were made.

Figure 1 is a plot of the percentage difference between the observed forward I_cs and the I_c averaged over all taps and observations at each magnetic field. For the data between 6 and 11 T, the variation of measured I_cs among the pairs of voltage taps was typical of specimen homogeneity. The indicated precision of the repeat determinations (indicated by multiple data points for the same tap at the same field) was also typical of these measurements. The lower group of data points at 12 T were the first measurements of this specimen and were made with forward current (Lorentz force in). The upper group of data points at 12 T were taken after reverse I_c (Lorentz force out) measurements were made (the data for reverse I_c is not shown on the plot). These 12 T data indicate an irreversible enhancement in the forward I_c which can also be seen in the (G–D)/D column of *Table 1* where a discontinuity exists betweeen 11 and 12 T. The limitations of varnish as a bonding agent are demonstrated by these results. First, the limited tensile strength of the varnish is incapable of constraining the wire on the mandrel even under moderate, outward Lorentz force. Second, even under compressive loads, the varnish seems incapable of reproducing the results obtained with epoxy. Sample inhomogeneity could also explain this difference.

Figure 2 is a semi-logarithmic plot of I_c *versus* magnetic field. A semi-logarithmic plot was selected because it illustrates the percentage differences between the curves. The central, thick curve is significantly lower than the others and the thin, varnish curve is slightly lower. *Figure 3* is a semi-logarithmic plot of n *versus* magnetic field. The significant element of this plot is the lower values of n for the central, thick curve at the higher magnetic fields. This is consistent with a strain degradation. The magnitude of the differences among the other curves is insignificant for this measurement variable. *Figure 4* is a plot of the percentage difference between reverse and forward I_c *versus* magnetic field. The thin, varnish curve illustrates the large strain effect, 13% at 12 T, when the sample is not adequately constrained to the mandrel. The smaller difference at 6 T was probably due to the decreased strain sensitivity at the lower magnetic field. The other curves illustrate the competition between the self-field effect, which is significant at the lower magnetic fields, and the strain effect, which is dominant at the higher magnetic fields. The maximum difference for the specimens bonded with epoxy was only 2% at 12 T which indicates that this bonding method is very positive.

Sample Y

A summary of the data on sample Y is given in *Table 2* and *Figures 5–9*. The centrally reacted specimens were

Table 2 Data on sample Y

Specimen	1	2	3	3	4	4
	Central thick	Central thick	Central thick	Central thin bored	Self thin	Self thin
$\mu_0 H$(T)	(A)	(B)	(C)	(D)	(E)	(F)
	Critical current (amperes) at 10 μV m^{-1}					
6	398.1	372.5	397.1	447.8	429.1	
7	332.7	311.0	333.1	377.6	359.2	
8	279.4	261.2	280.0	320.5	302.4	
9	235.0	220.0	235.3	272.9	255.7	
10		184.9	198.9	232.7	216.1	
11		154.8	166.9	198.3	182.1	182.9
12		128.6	139.1	168.1		153.4
	Sample mandrel dimensions					
	(A)	(B)	(C)	(D)	(E)	(F)
Wall (mm)	9.3	9.3	9.3	2.5	2.0	2.0
Rad. (mm)	15.6	15.6	15.6	15.6	15.6	15.6
ratio	60%	60%	60%	16%	13%	13%
	Intercomparison of critical current data					
$\mu_0 H$(T)	(A–C)/C	(B–C)/C	(C–D)/D		(E–D)/D	(F–D)/D
6	0.3%	−6.2%	−11.3%		−4.2%	
7	−0.1%	−6.6%	−11.8%		−4.9%	
8	−0.2%	−6.7%	−12.6%		−5.6%	
9	−0.1%	−6.5%	−13.8%		−6.3%	
10		−7.0%	−14.5%		−7.1%	
11		−7.2%	−15.8%		−8.2%	−7.8%
12		−7.5%	−17.3%			−8.7%

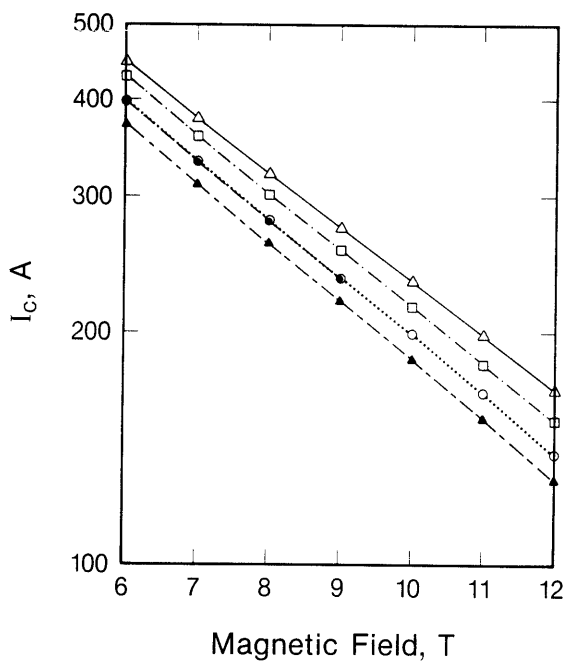

Figure 5 Semilogarithmic plot of I_c at 10 μV m^{-1} *versus* magnetic field for specimens of sample Y. $E_c = 10$ μV m^{-1}. ○ · · · ○, Central thick C; △——△, central bored; □–·–□, self thin; ●– – –●, central thick A; ▲– – –▲, central thick B

numbers 1, 2 and 3. With respect to mandrel geometry, mounting technique and the reaction site, these specimens were the same. Data sets A and C are in good agreement (0.3% maximum variation); however, set B is in contradiction with both A and C (7.5% maximum difference). There are several possible explanations for this discrepancy including shipping damage, mounting damage, sample inhomogeneity and variation in mandrel thermal contraction. These data are insufficient to determine the most likely source of this effect. Data set D was acquired on specimen 3 after boring and again is an indication of the pre-strain effect. The magnitude of this I_c enhancement was 17% at 12 T and is in approximate agreement with a 0.2% change in the pre-strain state of the wire as explained for sample X above. Sample Y's higher upper critical field would explain a lower strain sensitivity than that of sample X (39% at 12 T).

Data sets E and F, self reacted specimen number 4, are compared to data set D and again there is a similar I_c discrepancy (8.7% at 12 T) between two comparable specimens. The additional possible explanation for this is the fact that these specimens were reacted at different sites. A comparison of data sets E and F was another check on the effect of thermal cycling. These abbreviated data sets and resulting thermal cycles were the result of one of several magnet quenches and, as in the previous cases, the effect of thermal cycling on I_c appears to be about 0.4%.

The most significant result for this sample is, again, the dependence of I_c on mandrel wall thickness.

Figure 5 is a semi-logarithmic plot of I_c *versus* magnetic field. These curves show two data bands: an upper band, associated with the thin-walled specimens, and a lower band, associated with thick-walled specimens. While there is considerable variation in the curves, the dominant variation is between the thick and thin-walled mandrels. *Figure 6* is a semi-logarithmic plot of *n versus* magnetic field. The larger data scatter for the central thick C curve may be due to the tap-to-tap I_c variation observed on

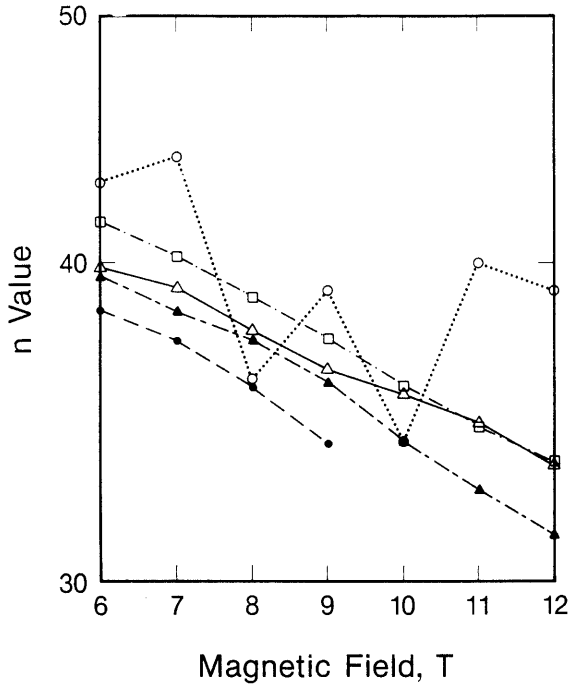

Figure 6 A semilogarithmic plot of *n* value *versus* magnetic field for specimens of sample Y. ○ · · · ○, Central thick C; △——△, central bored; □ - · - □, self thin; ●---●, central thick A; ▲———▲, central thick B

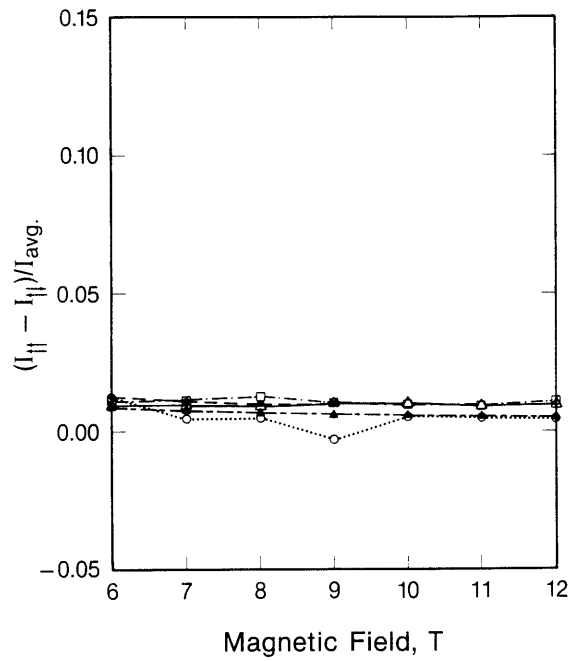

Figure 7 Percentage difference between I_c measured with reverse and forward current directions *versus* magnetic field for specimens of sample Y. $E_c = 10\,\mu V\ m^{-1}$. ○ · · · ○, Central thick C; △——△, central bored; □ - · - □; self thin; ●---●, central thick A; ▲———▲, central thick B

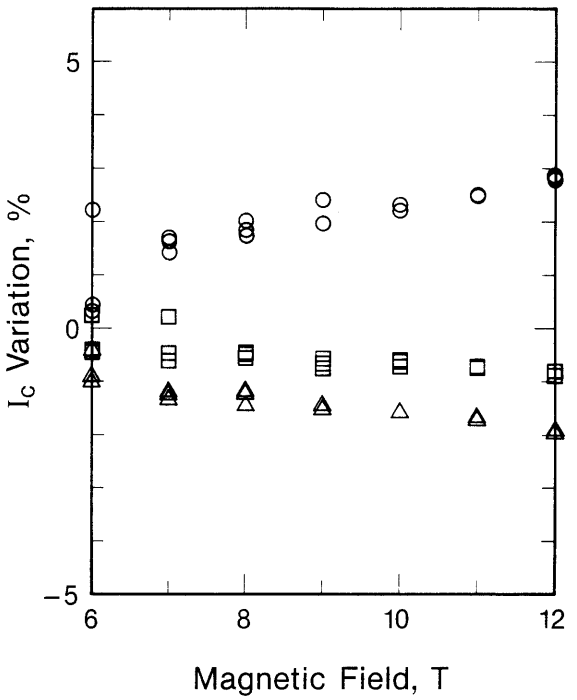

Figure 8 Percentage variation of I_c about the average I_c *versus* magnetic field for specimen C (central, thick) of sample Y. Tap symbols: ○, 1; □, 2; △, 3

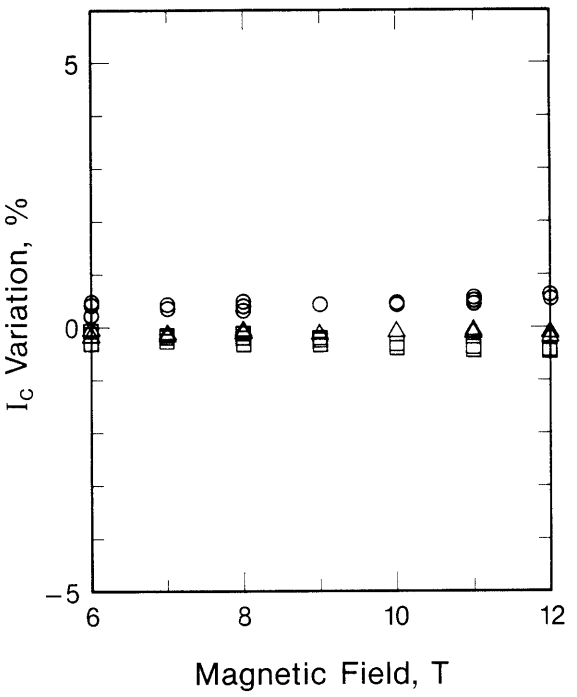

Figure 9 Percentage variation of I_c about the average I_c *versus* magnetic field for specimen D (central, thick, bored) of sample Y. Tap symbols: ○, 1; □, 2; △, 3

this specimen. The magnitude of the differences among the other curves is insignificant for this measurement variable. *Figure 7* is a plot of the percentage difference between forward and reverse I_c *versus* magnetic field. In this case the maximum difference was only about 1%. These curves are similar to those for sample X, *Figure 4*, and indicate that the specimen was well bonded to the mandrel.

Figures 8 and *9* are plots of the percentage difference between the observed forward I_cs and the I_c averaged over all taps and observations at each magnetic field. Both of these plots contain data for specimen 3, the

difference being that *Figure 8* contains central thick C data and *Figure 9* contains central thick-bored D data. The significant difference between the two plots is that the tap-to-tap I_c variation, observed in *Figure 8*, was not present after boring as shown in *Figure 9*. One possible explanation is a reduced longitudinal variation in G10 thermal contraction after boring. The variation of measured I_cs for the other specimens was similar to that of *Figure 9*.

Sample Z

A summary of the data on sample Z is given in *Table 3* and *Figures 10–12*. The centrally reacted specimens were numbers 1 and 2 with specimen 3 being self reacted. Data sets A, B, and C are in good agreement, with a 1.6% variation in I_c at 12 T. The centrally reacted specimens were measured on mandrels that had an outer diameter of about 19 mm rather than the typical 31 mm of all the other specimens. Prior to this study, this diameter was convenient for the anticipated measurements and not expected to be a significant variable. Given these limited data and this extra variable, no additional conclusion can be made regarding mandrel geometry and reaction site.

Figure 10 is a semi-logarithmic plot of I_c *versus* magnetic field. *Figure 11* is a semi-logarithmic plot of n *versus* magnetic field. The significant information contained in this plot is the relatively high n value for this conductor. *Figure 12* is a plot of the percentage difference between forward and reverse I_c *versus* magnetic field. In this case the maximum difference was only about 4%. With the possible exception of the self reacted specimen, these curves are similar to those for samples X and Y, *Figures 4* and *7*, and indicate that the specimen was well bonded to the mandrel. Within the limits of the measurement precision for this sample, homogeneity between taps was similar to the other samples.

Table 3 Data on sample Z

Critical current (amperes) at 10 μV m^{-1}			
Specimen	1	2	3
μ_0H(T)	Central (A)	Central (B)	Self (C)
6		544.1	
7		454.5	443.1
8		381.4	372.2
9		320.6	311.5
10	270.6	268.9	263.5
11	226.4	224.3	221.1
12	187.6	185.6	184.6
Sample mandrel dimensions			
	(A)	(B)	(C)
Wall (mm)	3.0	3.0	2.0
Rad. (mm)	9.3	9.3	15.6
ratio	32%	32%	13%
Intercomparison of critical current data			
μ_0H(T)	(A–B)/B		(C–B)/B
6			
7			−2.5%
8			−2.4%
9			−2.8%
10	0.6%		−2.0%
11	0.9%		−1.4%
12	1.1%		−0.5%

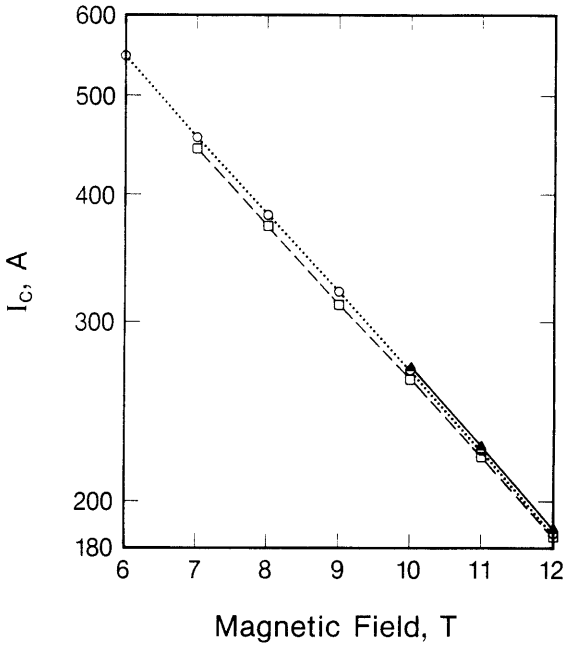

Figure 10 A semilogarithmic plot of I_c at 10 μV m^{-1} *versus* magnetic field for specimens of sample Z. $E_c = 10\ \mu V\ m^{-1}$. ▲——▲, Central A; ○ · · · ○, central B; □ – – – □, self

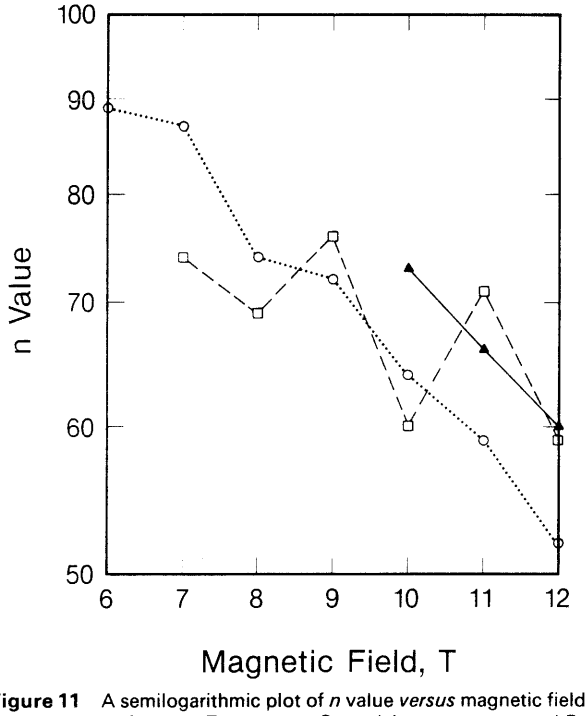

Figure 11 A semilogarithmic plot of n value *versus* magnetic field for specimens of sample Z. ▲——▲, Central A; ○ · · · ○, central B; □ – – – □, self

Thermal contraction measurements and strain calculations

Thermal contraction measurements on NEMA-type (National Electrical Manufacturers' Association) G10 glass–epoxy composites have been published for the plate

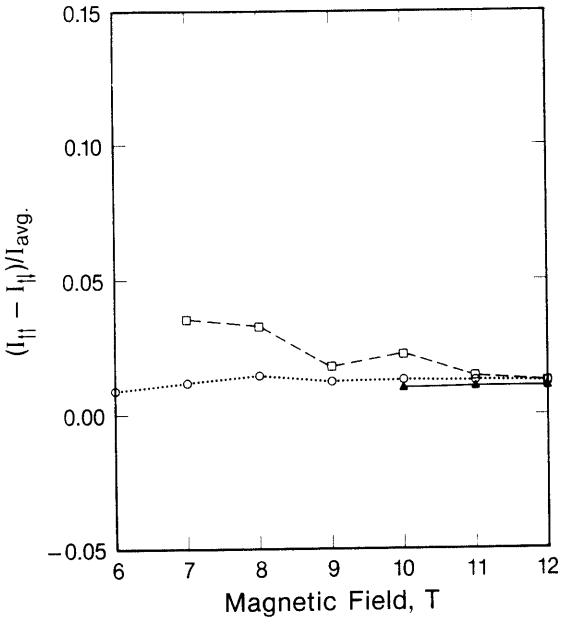

Figure 12 Percentage difference between I_c measured with reverse and forward current directions *versus* magnetic field for specimens of sample Z. $E_c = 10\,\mu V\ m^{-1}$. ▲——▲, Central A; ○ · · · ○, central B; □ – – – □, self

geometry[5–7] but not for the tube geometry. The contraction of a G10 plate is highly anisotropic. In composite nomenclature, the two directions in the plane of the fibreglass fabric are warp and fill. The direction perpendicular to the plane of the fabric is referred to as the normal direction. The thermal contraction from 293 K to 4 K is about 0.24% for the warp direction and 0.71% for the normal direction. The contraction in the fill direction is expected to be a little more than that of the warp direction. The contraction in the warp direction is dominated by the fibreglass fabric and the normal direction is dominated by the epoxy. The G10 tubes used for measurement mandrels were rolled spirals of fibreglass fabric embedded in an epoxy matrix, rather than tubes machined from plate material. The radial direction for a rolled tube is normal to the fabric. The radial contraction of a tube is different than the contraction of a plate, however, because the circumferential fibreglass is put in hoop compression by the epoxy and the resulting contraction is a competition between the two structural components. The dependence of the radial contraction on wall thickness is expected to be caused by this competition.

A subset of the round robin participants used measurement mandrels from a single batch of G10 tubes to reduce the number of measurement variables among these laboratories. A thick-walled G10 tube was originally selected as a common sample mandrel material to allow adaptation of one size tube to the various test fixtures. However, a thick-walled tube is difficult to manufacture without delaminations that can cause irregular contraction and voids when they are machined. Also, the outer diameter can change when the inner diameter is bored. Another observation was that the radial contraction can be slightly asymmetric; this will result in an approximately elliptical rather than circular cross section at low temperatures. In order to make an approximate correction for this, the thermal contraction measurements are the average of two approximately orthogonal measurements of the tube's diameter.

As briefly mentioned above, thermal contraction measurements were made on several G10 tubes in order to estimate the resulting conductor strain. In the interest of expediency, these measurements were limited both in accuracy and precision; nonetheless, the measurements give an indication of the variation in thermal contraction between the tubes. These tests consisted of measuring the outside diameter of the G10 tube at room temperature, submerging the tube in liquid nitrogen, allowing it to reach thermal equilibrium and then quickly removing it and remeasuring the diameter. These measurements were made with a precision micrometer but they were limited by the practical difficulties of the measurement. Two tube geometries were measured; both had 31.2 mm nominal outside diameters, but one tube had a 12.7 mm inside diameter while the other had a 26.2 mm inside diameter. These two geometries had 9.3 mm and 2.5 mm walls, respectively, and are representative of the thick- and thin-walled mandrels. These measurements showed a substantial difference between the radial thermal contraction of G10 tubes having different wall thicknesses. Specifically, the thin-walled tube's radial thermal contraction was ~0.23% while the thick-walled tube's contraction was ~0.41%. A bias in this study exists as a result of the thermally transient measurement conditions (with a systematic difference in thermal mass) and the fact that it was conducted at liquid nitrogen, rather than liquid helium, temperature. Both of these factors result in an underestimation of the actual thermal contraction between room and liquid helium temperatures. Based on the temperature dependence of the thermal contraction of G10 plate[5,6], the thermal contraction to 4 K was estimated as ~0.28% for the thin-walled tube and ~0.48% for the thick-walled tube. The thermal contraction of the Nb_3Sn conductor was only ~0.21%; consequently, the G10 contraction may have introduced additional amounts of conductor pre-strain. The amount of compressive pre-strain might depend on several factors including the mandrel's wall thickness and the strength of the mandrel-to-conductor bond.

For samples X and Y, considerable I_c tensile-strain-sensitivity data were available; however, no explicit data were available for compressive strain sensitivity. Consequently, the strain scaling law[3] in conjunction with the available tensile strain data was used to estimate the expected I_c degradation for compressive strain. For sample X the results of these calculations predict a ~33% reduction in the I_c at 12 T for the thick-walled specimens as compared to the thin-walled ones. As mentioned above, the observed reduction was ~39%. Sample Y had a lower strain sensitivity with a predicted I_c degradation of ~24% at 12 T. The actual reduction in I_c for the thick mandrel as compared to the thin was ~18%. As stated above, these measurements and calculations are only approximate but the trend seems to be obvious. In all cases, the thick-walled samples had reduced I_cs and this reduction was in approximate agreement with that predicted by the strain scaling law.

Discussion

Sample damage is a major concern because it can go undetected and have a significant effect on the accuracy

of the I_c measurement. Two potential sources of damage are shipping, when the packaging of reacted samples is inadequate, and sample transfer from the reaction mandrel to the measurement mandrel, particularly when diffusion bonding between the specimen and the stainless steel reaction mandrel has occurred.

Diffusion bonding has been observed even in cases where the surface of the stainless steel was oxidized prior to sample reaction. Consequently, a more complete and reliable technique for oxidizing the reaction mandrel needs to be developed. If specimen damage during transfer is to be avoided, dexterity and patience are required. Unthreading the specimen from a grooved mandrel seems to be better than attempting to flex the coil to a larger diameter in order to slip it over the grooves. Long coils tend to tighten as they are unthreaded unless the torque is evenly distributed among the coil turns during the process.

The other potential source of sample damage, shipping, is more easily avoided. Careful packaging of the samples can eliminate concerns over shipping damage. The reaction mandrel alone cannot protect a sample from shipping damage. The packaging needs to protect the sample from collisions with external objects as well as from inertial collisions with other specimens within the container or with the container itself.

Within this study it was not possible to separate the effect of reaction variables or sample inhomogeneity from that of shipping damage; however, considering the poor packaging that was used for some of the samples, it is suspected that sample damage may have played a role in these measurements. The damage or loss of samples during shipping and the delay of sample shipments by customs are characteristic problems of international round robin measurements and, hopefully, with experience these problems will be reduced.

The study concerning the effect of boring and thick-*versus* thin-walled G-10 tubes was not originally intended but, rather, the results of initial measurements led naturally to it. Thus, the number of specimens and the schedule limited the completeness and organization of these results. A more selective data presentation was not used because it would imply that there were fewer difficulties and that less was learned in these studies than was actually the case.

A round robin is a unique measurement setting where the interlaboratory comparison of results is essential to the advancement of measurement accuracy. Although only the NBS results have been presented herein, it was the preliminary comparison between these results and results from the other laboratories that lead to the expansion of the NBS study and, ultimately, to the source of the measurement discrepancies.

Conclusions

Two major conclusions are that the bonding method and the mandrel material and geometry have a significant effect on the critical current measurement of Nb_3Sn. Thick wall G10 tubes contract about 0.2% more than thin wall G10 from room to liquid helium temperature. Thus, the amount of differential thermal contraction between the mandrel and the sample depends on the wall thickness of the G10. The method of bonding the sample to the mandrel also determines how much of the differential thermal contraction is transmitted to the sample. A positive bond will change the strain state of the sample more than a weak bond; however, a weak bond may allow the sample to be strained by the Lorentz force. The difference between critical current measurements on thick and thin wall G10 was about 20% at 12 T for a Nb_3Sn conductor with an upper critical field of 24 T and about 35% at 12 T for one with an upper critical field of 19 T.

The effect of self *versus* central sample reaction was not indicated as a major source of error in the resulting critical current measurements. The most direct comparison of this effect can be made on sample X, where the effect was less than 3% at 12 T. Furthermore, sample X should have been more sensitive to reaction conditions because of its relatively short reaction time, which may not have fully reacted the Nb filaments.

Some preliminary recommendations based on these results can be made. G10 tubes with wall thickness less than about 20% of the tube radius are well matched in thermal contraction to Nb_3Sn wires and use of this type of tube for measurement mandrels should result in a minimum of conductor strain. The boring of thick-walled G10 tubes for use as measurement mandrels may, due to structural voids, result in irregular thermal contraction. A well oxidized stainless steel reaction mandrel should be used to reduce diffusion bonding of the sample to the reaction mandrel and the possibility of damage when the sample is transferred to the measurement mandrel. A thin, continuous coat of epoxy will provide a good bond between the sample and the mandrel; however, in cases where end cooling of the sample is inadequate, this method may result in a lower measured I_c. Also, from a practical standpoint other bonding materials, such as varnish or grease, that are easily removed from the measurement mandrel may be preferable to epoxy for routine measurements. These bonding materials may be adequate in cases where the measurements are conducted with the Lorentz force into the mandrel.

The results presented here are preliminary in the sense that they have yet to be correlated with measurements from all 24 participating laboratories. This correlation is a necessary element in a study of this type and may clarify the results presented here. The effect of thick- *versus* thin-walled measurement mandrels discovered in this study indicates that in order for various laboratories to arrive at the same I_c results, a more detailed unification of the measurement techniques would be required. However, this would not ensure the correctness of the results, only a consistency of results. A unified definition of the desired measurement, aimed at achieving the maximum usefulness and practicality of the resulting data, is required in order to make a correct measurement. Hopefully, a future joint publication will address some of these issues and result in a simple measurement method that has only the restrictions necessary to achieve this end.

Acknowledgements

The authors extend their thanks to J.W. Ekin for discussions on these results, to R.M. Folsom and T.C. Stauffer for sample preparation, data reduction and plotting, to D.L. Rule for help with data plotting, to W.E. Look for assistance with the magnetic field calibration and to the other VAMAS participants.

This work was supported by the Department of Energy, Office of Fusion Energy and Division of High Energy Physics.

An effort was made to avoid the identification of commercial products by the manufacturer's name or label, but in some cases these products might be indirectly identified by their particular properties. In no instance does this identification imply endorsement by the National Bureau of Standards, nor does it imply that the particular products are necessarily the best available for that purpose.

References

1 **Goodrich, L.F. and Fickett, F.R.** Critical current measurements: a compendium of experimental results *Cryogenics* (1982) **22** 225

2 Standard Test Method for D-C Critical Current of Composite Superconductors *Annual Book of ASTM Standards* ASTM B714-82, Part 02.03, American Society for Testing and Materials, Philadelphia, PA, USA (1983) 595–598

3 **Ekin, J.W.** Strain scaling law for flux pinning in practical superconductors. Part 1: Basic relationship and application to Nb_3Sn conductors *Cryogenics* (1980) **20** 611

4 **Bray, S.L., Goodrich, L.F. and Dube, W.P.** Battery powered current supply for superconductor measurements *Rev Sci Inst* (1989) **60** 261

5 **Fujii, G., Ekin, J.W., Radebaugh, R. and Clark, A.F.** Effect of thermal contraction of sample holder material on critical current *Adv Cryog Eng Mater* (1980) **26** 589

6 **Fujii, G., Ranney, M.A. and Clark, A.F.** Thermal expansion of Nb_3Sn and V_3Ga multifilamentary superconducting cables, fiberglass–epoxy and cotton–phenolic composite materials *Jap J Appl Phys* (1981) **20** L267

7 **Clark, A.F., Fujii, G. and Ranney, M.A.** The thermal expansion of several materials for superconducting magnets *IEEE Trans Magn* (1981) **MAG-17** 2316